

## ORIGINAL ARTICLE

## Ibrutinib-induced lymphocytosis in patients with chronic lymphocytic leukemia: correlative analyses from a phase II study

SEM Herman<sup>1,5</sup>, CU Niemann<sup>1,5</sup>, M Farooqui<sup>1,5</sup>, J Jones<sup>1,2</sup>, RZ Mustafa<sup>1</sup>, A Lipsky<sup>1</sup>, N Saba<sup>1</sup>, S Martyr<sup>1</sup>, S Soto<sup>1</sup>, J Valdez<sup>1</sup>, JA Gyamfi<sup>1</sup>, I Maric<sup>3</sup>, KR Calvo<sup>3</sup>, LB Pedersen<sup>4</sup>, CH Geisler<sup>4</sup>, D Liu<sup>1</sup>, GE Marti<sup>1</sup>, G Aue<sup>1</sup> and A Wiestner<sup>1</sup>

Ibrutinib and other targeted inhibitors of B-cell receptor signaling achieve impressive clinical results for patients with chronic lymphocytic leukemia (CLL). A treatment-induced rise in absolute lymphocyte count (ALC) has emerged as a class effect of kinase inhibitors in CLL and warrants further investigation. Here we report correlative studies in 64 patients with CLL treated with ibrutinib. We quantified tumor burden in blood, lymph nodes (LNs), spleen and bone marrow, assessed phenotypic changes of circulating cells and measured whole-blood viscosity. With just one dose of ibrutinib, the average increase in ALC was 66%, and in >40% of patients the ALC peaked within 24 h of initiating treatment. Circulating CLL cells on day 2 showed increased Ki67 and CD38 expression, indicating an efflux of tumor cells from the tissue compartments into the blood. The kinetics and degree of the treatment-induced lymphocytosis was highly variable; interestingly, in patients with a high baseline ALC the relative increase was mild and resolution rapid. After two cycles of treatment the disease burden in the LN, bone marrow and spleen decreased irrespective of the relative change in ALC. Whole-blood viscosity was dependent on both ALC and hemoglobin. No adverse events were attributed to the lymphocytosis.

*Leukemia* (2014) 28, 2188–2196; doi:10.1038/leu.2014.122

## INTRODUCTION

Chronic lymphocytic leukemia (CLL), a malignancy of mature B-cells that involves blood, bone marrow and lymphoid tissues, is the most common leukemia in Western countries.<sup>1</sup> In the United States alone, ~120 000 people live with CLL,<sup>2</sup> while an estimated 15 680 people will be newly diagnosed with and 4580 will die of CLL in 2013.<sup>3</sup> Median survival with early stage disease is 10.7 years; however, the clinical course is quite heterogeneous, depending on prognostic markers like immunoglobulin heavy chain variable (*IGHV*) gene mutation status, ZAP70 expression, deletion of the short arm of chromosome 17 (del(17p)) or the presence of SF3B1 and NOTCH1 mutations.<sup>4,5</sup>

B-cell receptor (BCR) signaling has emerged as a key pathway in the pathogenesis of CLL.<sup>6–8</sup> A role for antigenic stimulation of the clonal cells was first indicated by the observation that CLL cells use a restricted repertoire of *IGHV* genes that encode the antigen-interacting interface of the BCR.<sup>9,10</sup> More recently, the discovery of BCR stereotypes shared by a substantial proportion of CLL cases suggests that CLL cells may arise from B-cells with defined antigen specificities.<sup>11,12</sup> BCR signaling and activation of the NF- $\kappa$ B pathway occur primarily in the lymph node (LN) microenvironment promoting cell growth, proliferation, and survival.<sup>13,14</sup> Thus, antigenic stimulation emerges as a driving pathway in the pathogenesis of CLL; a mechanism that is also implicated in an increasing number of mature B-cell malignancies.<sup>15,16</sup>

Bruton's tyrosine kinase (BTK), a cytoplasmic non-receptor tyrosine kinase, is recruited early in the BCR signaling cascade in conjunction with SYK and phosphatidylinositol 3'-kinase  $\delta$ .<sup>16,17</sup> BTK couples BCR activation to intracellular calcium release and

activation of nuclear factor- $\kappa$ B and is essential for normal B-cell development and response of B-cells to antigenic stimulation.<sup>18</sup> Knockdown of BTK is lethal to select lymphoma cell lines derived from activated B-cell-like diffuse large B-cell lymphoma<sup>19</sup> and decreases the viability of primary CLL cells.<sup>20</sup> In addition, genetic ablation of BTK inhibits disease progression in mouse models of CLL.<sup>20,21</sup> Ibrutinib, an orally active agent, covalently binds to Cys-481 of BTK, thereby irreversibly inactivating the kinase.<sup>22</sup> In the phase I study, ibrutinib was well tolerated and active across a spectrum of mature B-cell malignancies, with the highest response rates in CLL and mantle cell lymphoma.<sup>23,24</sup> More recently, overall response rates of >70%, and an estimated 26-month progression-free survival rate of 75% for previously treated patients with CLL was reported.<sup>25</sup> *In vitro* ibrutinib has been shown to inhibit proliferation, adhesion and migration of CLL cells.<sup>26–29</sup> Further, murine CLL models suggest that ibrutinib inhibits homing of CLL cells to tissue sites.<sup>28,30</sup>

In addition to ibrutinib, several other inhibitors of kinases in the BCR pathway are in clinical development.<sup>7,8,16,31</sup> Initial clinical experience with such BCR inhibitors raised concerns owing to a sometimes dramatic worsening of peripheral lymphocytosis,<sup>32,33</sup> which is now recognized as a class effect. Concerns about patient safety due to the treatment-induced lymphocytosis have been somewhat alleviated by the increasing experience with these agents in clinical trials. However, many questions remain. Here we focused on the kinetics and inter-individual variability in treatment-induced lymphocytosis, characterized changes in the immune-phenotype of circulating CLL cells on treatment, assessed concomitant changes in disease distribution in different

<sup>1</sup>Hematology Branch, National Heart, Lung, and Blood Institute, National Institutes of Health, Bethesda, MD, USA; <sup>2</sup>Medical Research Scholars Program, National Institutes of Health, Bethesda, MD, USA; <sup>3</sup>Department of Laboratory Medicine, Clinical Center, National Institutes of Health, Bethesda, MD, USA and <sup>4</sup>Department of Hematology, Rigshospitalet, Copenhagen University Hospital, Copenhagen, Denmark. Correspondence: Dr A Wiestner, Hematology Branch, National Heart, Lung, and Blood Institute, National Institutes of Health, Building 10, Room 8c104, CRC 3-5140 10 Center Drive, Bethesda, MD 20892-1202, USA.  
E-mail: wiestnea@nhlbi.nih.gov

<sup>5</sup>These authors contributed equally to this work and are co-first authors.

Received 6 January 2014; revised 21 February 2014; accepted 21 March 2014; accepted article preview online 4 April 2014; advance online publication, 6 May 2014

anatomical compartments and sequentially determined whole-blood viscosity during the period of peak lymphocytosis. We found that the ibrutinib-induced lymphocytosis developed almost immediately after the first dose of drug, peaked within 24 h in many patients and showed pronounced inter-patient variability. We provide direct *in vivo* evidence that the initial rise in lymphocytosis is in large part due to the release of previously activated cells from the LN. Furthermore, substantial reductions in tumor burden in the LN, bone marrow and spleen independent of changes in the number of circulating CLL cells underscores the notion that in CLL patients treated with BCR inhibitors the ALC is not a valid surrogate of overall disease burden or activity.<sup>32</sup>

## MATERIALS AND METHODS

### Patients, blood counts and whole-blood viscosity

We report correlative analyses on 64 CLL patients enrolled between January 2012 and October 2013 in our ongoing, investigator-initiated phase II study of ibrutinib (NCT01500733). The study was approved by the local ethics committee; informed consent was obtained from all patients in accordance with the Declaration of Helsinki. Briefly, both treatment naïve and relapsed/refractory patients with either del(17p) or age  $\geq 65$  years were eligible (Table 1) and treated with ibrutinib 420 mg orally once daily until disease progression or the occurrence of intolerable side effects. Mutation status of the *IGHV* gene was assessed as described, and CLL with  $< 2\%$  mutations was classified as unmutated.<sup>13</sup> Complete blood counts were determined in the NIH central laboratory. Groups of patients having distinct patterns of treatment-induced lymphocytosis (with regards to degree of change in ALC and the kinetics of onset and resolution) were identified using hierarchical clustering (Eisen Laboratory, Stanford University, Stanford, CA, USA). Whole-blood viscosity was determined by quantitative viscometry of whole blood (ARUP Laboratories, University of Utah, Salt Lake City, UT, USA). Adverse events were graded according to CTCAE v 4.03.

### Modeling CLL tumor burden and tissue redistribution

Tumor volume in the spleen and LN was computed from computed tomography scans using the syngovia software (Siemens, Cary, NC, USA). Of the spleen volume, 70% was considered due to CLL cells.<sup>34</sup> Bone marrow volume was calculated as previously published<sup>35</sup> and the content of CLL cells was calculated from the overall marrow cellularity multiplied by the degree of CLL cell infiltration. Cellular density was estimated at  $10^9$  cells/ml based on measurements of thymocyte density.<sup>36</sup> Peripheral blood (PB) volume was calculated using the Nadler formula.<sup>37</sup> The number of CLL cells was calculated based on measured ALC and the percentage of CD19<sup>+</sup> cells among all lymphocytes.

**Table 1.** Patient characteristics

	n	Sex (% M)	Rai stage (% 3,4)	% IGHV unmutated <sup>a</sup>	% CD38 <sup>+</sup> <sup>b</sup>	Median pre-ALC
> 65 years						
TN	14	57	64	45	29	142
RR <sup>c</sup>	15	47	80	71	64	96
del(17p)						
TN <sup>c</sup>	24	54	63	53	22	74
RR	11	55	64	7	36	94
All <sup>c</sup>	64	58	70	61	37	93

Abbreviations: ALC, absolute lymphocyte count; IGHV, immunoglobulin heavy chain variable; M, male; RR, relapsed/refractory; TN, treatment naïve. <sup>a</sup>Unmutated indicates  $< 2\%$  change in *IGHV* gene sequence compared with germline. <sup>b</sup>CD38 positive (+) indicates that  $\geq 30\%$  of chronic lymphocytic leukemia cells express CD38 above isotype control. <sup>c</sup>One patient in the >65-year RR group and six patients in the del(17p) group do not have available *IGHV* mutational information or CD38 expression data. Shown are the percentages of the patients where information was available. TN: patients who are treatment naïve; RR: patients who are refractory or have relapsed after one or more treatments.

### Flow cytometry

Peripheral blood mononuclear cells were prepared by density-gradient centrifugation (Lymphocyte Separation Media; ICN Biomedicals, Irvine, CA, USA). LN-derived single-cell suspensions were obtained from core biopsies. Cell suspensions were stained as previously described (BD Biosciences, Franklin Lakes, NJ, USA).<sup>30</sup> For Ki67 staining, cells were fixed in 4% paraformaldehyde and permeabilized in 70% EtOH. To assess cell death, fresh whole-blood samples were collected, red cells were removed by ACK lysis and CLL cell viability was assessed with the LIVE/DEAD Fixable Violet Dead Cell Stain Kit (Invitrogen, Grand Island, NY, USA). Cells were analyzed on a FACS Canto II flow cytometer (BD Biosciences) using the FACS-DIVA 6.1.1 and FlowJo software (Version 8.8.6; TreeStar, Ashland, OR, USA).

### Statistical analysis and mathematical modeling

When comparing the patient groups, a linear model was applied (JMP10 software, SAS Inc, Cary, NC, USA). When comparing specific events among the patient groups, a Fisher's exact test was used. All other statistical analyses were by Student's *T*-test (Prism5, GraphPad, La Jolla, CA, USA).

To test the hypothesis that the treatment-related increase in ALC is due to efflux of CLL cells from the LN, the predicted percentage of CLL cells expressing Ki67 (Ki67<sub>PB</sub>) on day 2 was calculated from the change in ALC and the measured percentage of CLL cells expressing Ki67 before treatment in PB (Ki67<sub>PB</sub> pre) and LN (Ki67<sub>LN</sub> pre):

$$\text{Ki67}_{\text{PB Day 2}} = \left( \frac{\text{ALC pre}}{\text{ALC Day 2}} \right) \text{Ki67}_{\text{PB pre}} + \left( 1 - \frac{\text{ALC pre}}{\text{ALC Day 2}} \right) \text{Ki67}_{\text{LN pre}}$$

## RESULTS

Ibrutinib-induced lymphocytosis develops within hours of starting treatment and is highly variable between patients

Within 24 h of initiating ibrutinib, the mean baseline ALC of 105 000/ $\mu\text{l}$  increased on average by 66% ( $P < 0.001$ ) and continued to increase throughout the first cycle before it gradually declined (Figures 1a and b). Within 4 h of starting the treatment, the mean ALC had already increased in most patients (data not shown). Thus the onset of ibrutinib-induced lymphocytosis was virtually immediate and in many patients reached its peak within days; in 46% of patients on day 2 and in 78% by day 28 (Figure 1c). The magnitude of the treatment-induced lymphocytosis was highly variable between patients (Figure 1d), without any correlation to previous treatment history or the presence or absence of del(17p) (Supplementary Figures S1a–d). However, patients with *IGHV*-mutated CLL showed a more pronounced rise in ALC that resolved more slowly than in patients with *IGHV*-unmutated CLL ( $P < 0.001$ ; Supplementary Figures S1e and f).

To test for factors that might predict distinct patterns of lymphocytosis, we used an unsupervised clustering analysis of the relative change in ALC over the first 6 months on treatment compared with baseline. Three separate clusters of patients that differ in the degree and the kinetics of the lymphocytosis were identified (Figures 2a–c). Notably, the pretreatment ALC was significantly different among the three clusters ( $P < 0.002$ , Figure 2d). The mean pretreatment ALC was highest for patients in cluster 1, and in this group of patients, the treatment-induced lymphocytosis peaked within days and resolved rapidly. Conversely, patients in cluster 3 tended to have lower pretreatment ALC and showed a greater relative increase in lymphocytosis that developed and resolved more slowly. Compared with the other clusters, cluster 3 was enriched for patients having *IGHV*-mutated CLL and bulky lymphadenopathy (at least one node with largest diameter  $> 5$  cm; Table 2). Conversely, patients in cluster 1 frequently had advanced Rai stage (80%). Thus, it appears that CLL patients with moderate lymphadenopathy may have a shorter time to peak ALC and a faster resolution of lymphocytosis, whereas bulky disease was associated with more prolonged lymphocytosis. Notably, there was no significant difference in the degree of nodal response at 6 months among the three clusters (Table 2), suggesting that a prolonged lymphocytosis does not

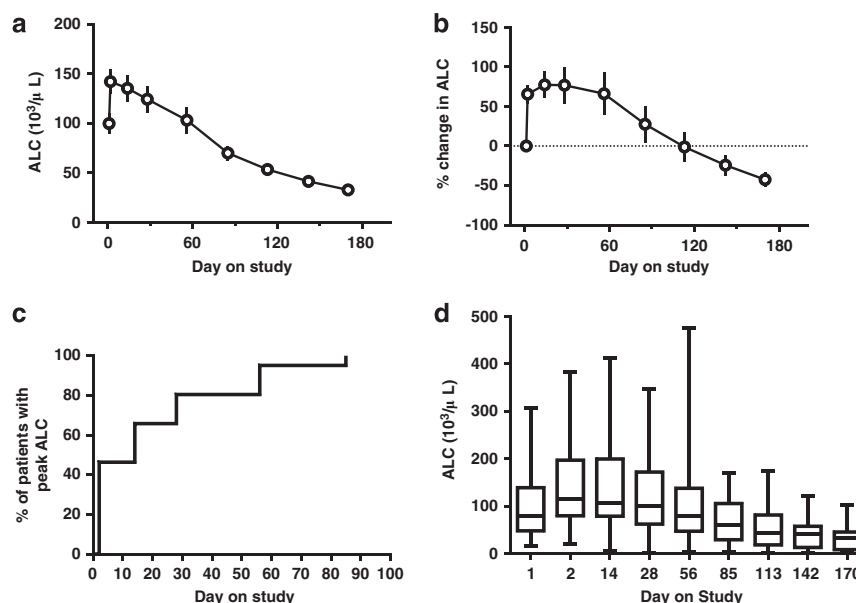


**Figure 1.** Ibrutinib-induced lymphocytosis develops rapidly, peaks within days and is highly variable between patients. (a–d) Data on 41 patients with complete counts for the first 6 months on ibrutinib are depicted. (a) Change in mean ALC over time; vertical lines indicate s.e.m. (b) Mean relative change of ALC on treatment over baseline; vertical lines indicate s.e.m. (c) Cumulative proportion of patients reaching their peak ALC at the indicated time points. Note: >40% of patients reached the peak ALC on day 2. (d) Box and whisker plots demonstrating distinct inter-patient variability in ALCs.

predict for inferior response, in agreement with a recent report by Woyach *et al.*<sup>38</sup>

Concurrent reduction in total tumor burden irrespective of treatment-induced lymphocytosis

We estimated a patient's total disease burden from the ALC, the extent of lymphadenopathy and splenomegaly on computed tomography scans and the degree of bone marrow infiltration. Figure 3 summarizes data for four representative patients. The distribution of disease among the different anatomical compartments varied greatly between individual patients (Figure 3a, Supplementary Table S1). During treatment, we repeatedly assessed the tumor burden in these sites for four patients chosen to represent cases with both diverse involvement of the four compartments before treatment and different kinetics of the treatment-induced lymphocytosis. The aggregate volume of lymphadenopathy as calculated from the computed tomography scans is shown for a representative patient in Figure 3b; ibrutinib reduced the pretreatment LN volume of 3161 ml (equal to an estimated  $3.2 \times 10^{12}$  CLL cells) by >80% within 2 months, with continued improvement at 6 months. Similarly, ibrutinib also rapidly reduced the tumor burden in the spleen (Figure 3c). The degree of bone marrow infiltration was estimated from anti-CD79a-stained bone marrow biopsies (Figure 3d). Irrespective of the initial tumor distribution, all four representative patients showed a pronounced decrease in the number of CLL cells over time, with the most rapid decrease occurring during the first 2 months (Figure 3e). One patient showed an apparent increase in the total number of CLL cells at 2 months despite reductions in disease burden in all three tissue sites owing to a pronounced increase in ALC. This likely reflects release of CLL cells from the liver and intestinal tract, sites known to be significant reservoirs of B-cells but not included in our model.<sup>39–41</sup>

The substantial reduction in total tumor burden cannot be explained by mere disease redistribution between different anatomical sites and suggests that there is a substantial amount of treatment-induced cell death. For example, in three of the four patients shown in Figure 3e trillions of CLL cells 'disappear' within

the first 3 months; and that is only from the four sites amenable to study. However, evidence of cell death has been elusive. For example, none of the patients in our study showed signs of tumor lysis syndrome, and in ficoll, viably frozen PB mononuclear cells we failed to detect an increase in cell death or apoptosis. When we switched to analyzing fresh whole-blood samples, we found that before treatment a median 2.4% of the circulating tumor cells were dead or dying. On day 28 on ibrutinib, the frequency of dead or dying cells in circulation on average more than doubled compared with pretreatment ( $P = 0.03$ ; Figure 3f).

Evidence for efflux of tissue-resident CLL cells into the PB

*In vitro* and murine studies suggest that both inhibition of cell adhesion and homing of circulating cells to tissue sites may contribute to treatment-induced lymphocytosis in CLL.<sup>26–28,30</sup> Based on the rapid onset of the treatment-induced lymphocytosis, we hypothesized that efflux of CLL cells from tissue sites fuels the rise in circulating cells. To distinguish CLL cells in circulation from tissue-resident cells, we made use of previous observations that CLL cells are activated and proliferate in the tissue microenvironment, and that the two populations therefore differ in their immuno-phenotypic characteristics (Figure 4a).<sup>13,42,43</sup> Expression of activation markers, including CD38, CD69 and CD86, and the proliferation marker Ki67 have been found to be downregulated by BCR inhibitors.<sup>44–47</sup> As expected, we found downregulation of these markers on circulating tumor cells on day 14 of ibrutinib therapy (data not shown). However, on day 2, concurrent with the increase in ALC, the frequency of CD38 and Ki67-positive CLL cells in circulation increased significantly ( $P \leq 0.004$ , Figures 4b and c, and Supplementary Figure S2a), consistent with an influx of tissue-resident cells into the blood. Next we used the relative change in ALC and in the fraction of circulating cells expressing Ki67 on day 2 to estimate to what degree the influx of tissue-resident cells can account for the rise in ALC. Figure 4d illustrates these changes in a representative patient. The fraction of Ki67-expressing CLL cells as measured by flow cytometry before treatment was 6.4% in the PB and 12.8% in the LN. On day 2, the ALC had increased from 90 000/ $\mu$ L to

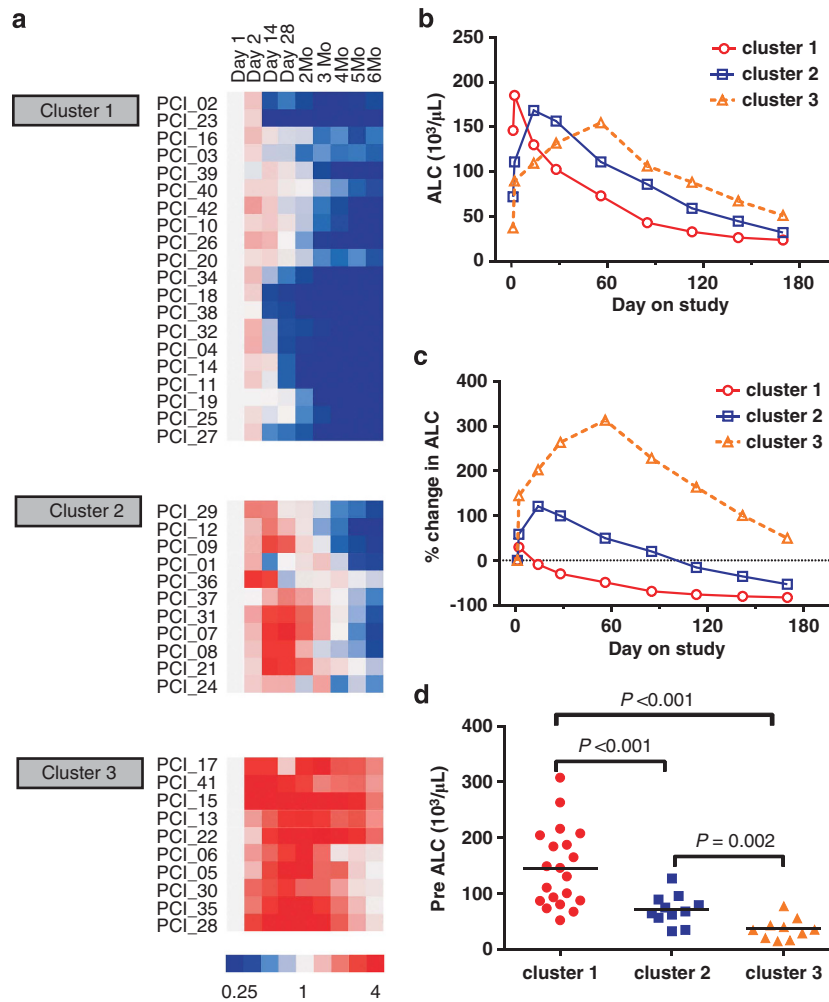


**Figure 2.** Variability in development and resolution of ibrutinib-induced lymphocytosis. **(a)** Hierarchical clustering of change in ALC normalized to baseline (day 1) in individual patients ( $n = 41$ ) reveals three distinct patterns. The degree of change is color coded according to the legend shown. **(b, c)** The mean for each of the three patient clusters is shown as **(b)** ALC or **(c)** relative change of ALC compared with pretreatment. **(d)** The pretreatment ALC for the three patient clusters are significantly different by Student's *T*-test.

**Table 2.** Characteristics of patients by cluster<sup>a</sup>

n	Treatment history (% TN)	Sex (% male)	Rai stage (% 3,4)	% IGHV unmutated <sup>b</sup>	% del(17p)	% CD38+ <sup>c</sup>	% Bulky disease <sup>d</sup>	Median age (years)	Median pre-ALC ( $10^9/\text{L}$ )	Median percentage of LN reduction (6 months)
Cluster 1 20	40	60	80	70	45	30	15	69	139	69
Cluster 2 11	55	64	73	55	55	45	55	67	68	78
Cluster 3 10	40	30	40	30	50	50	80	66	36	77

Abbreviations: ALC, absolute lymphocyte count; IGHV, immunoglobulin heavy chain variable; LN, lymph node; TN, treatment naive. <sup>a</sup>Clusters were determined by unsupervised hierarchical clustering as depicted in Figure 2a. <sup>b</sup>Unmutated indicates <2% change in IGHV gene sequence compared with germline. <sup>c</sup>CD38 positive (+) indicates that  $\geq 30\%$  of chronic lymphocytic leukemia cells express CD38 above isotype control. <sup>d</sup>Bulky disease was defined as patients with at least one lymph node measurement > 5 cm.

128 000/ $\mu\text{L}$ . Thus one-third of the cells on day 2 were 'additional cells'. If all these additional cells are derived from the LN, the frequency of Ki67-positive cells is predicted to increase to 8.3%.

Indeed, the actual frequency measured by flow cytometry was 8.2%. We could assess eight patients in this manner, and consistently, actual and predicted frequency of Ki67-expressing



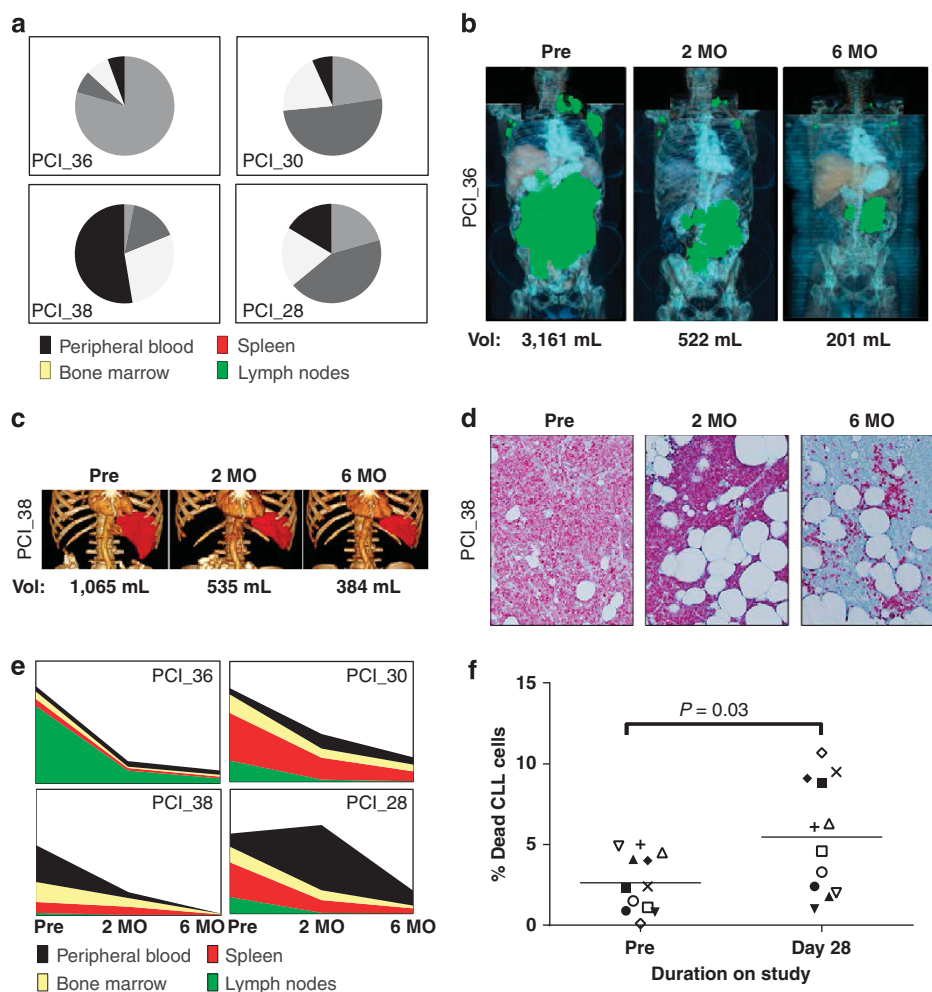


**Figure 3.** Ibrutinib rapidly decreased total tumor burden and increases the rate of cell death. **(a)** A graphic representation of the estimated tumor burden in different anatomic compartments before treatment is shown for four representative patients (identified by study code). **(b–d)** Change in tumor burden from pretreatment (Pre) to 2 and 6 months (MO) of treatment in different tissues. **(b)** Graphic representation of total LN volume computed from whole-body computed tomography (CT) scans. **(c)** Graphic representation of spleen volume computed from CT scan. **(d)** CLL cell infiltration of bone marrow visualized by CD79a staining. **(e)** Changes in disease burden on treatment is shown for the four representative patients. Also, see Supplementary Table S1. **(f)** The viability of circulating CLL cells was measured in fresh whole-blood samples using the LIVE/DEAD stain ( $n = 12$ , each symbol represents a different patient). Ibrutinib doubles the rate of cell death ( $P = 0.03$  by paired Student's *T*-test).

cells were virtually identical ( $R = 0.99$ ,  $P < 0.001$ ; Figure 4e). Using this same formula, we could also predict the expected rise in ALC based on the pretreatment and day-2 Ki67 values ( $R = 0.99$ ,  $P < 0.001$ ; Figure 4f). Thus, the treatment-induced rise in ALC on day 2 can be accounted for by the influx of LN-resident CLL cells into the blood.

Whole-blood viscosity is determined by ALC and hemoglobin. Patients with certain types of leukemia may develop leukostasis leading to central nervous system and respiratory impairment.<sup>48</sup> CLL patients, even those with very high lymphocyte counts, are rarely reported to suffer such complications; however, the rapid increase in ALC and the release of more activated cells from tissue sites might contribute an additional risk. Fortunately, no adverse events were attributed to leukostasis or hyperviscosity syndrome in this study, where the highest ALC was 475 000/ $\mu$ L, and 42% of patients had an ALC  $> 200$  000/ $\mu$ L at least once during the first 2 months. Prospectively measured whole-blood viscosity before treatment and on days 2 and 28 correlated with ALC but did so even more strongly with hemoglobin ( $P < 0.001$ , Figures 5a and b). Overall, there was no significant increase in whole-blood

viscosity on treatment (Figure 5c). Only in two patients a slightly increased whole-blood viscosity was recorded, in one patient on day 2 with an ALC of 405 000/ $\mu$ L and in the other on day 28 with an ALC of 388 000/ $\mu$ L. ALC and hemoglobin were inversely correlated, and patients with high ALC tended to be more anemic (Supplementary Figure S3). Interestingly, in patients with a pretreatment hemoglobin  $\geq 10$  g/dL, there was a decrease in mean hemoglobin from 11.7 to 10.9 g/dL during the first 28 days on treatment ( $P \leq 0.02$ , Figure 5d). Figure 5e illustrates the interaction of hemoglobin and ALC on whole-blood viscosity. Notably, the effect of a high ALC may in part be offset by a degree of anemia.

## DISCUSSION

Treatment-induced lymphocytosis has become a hallmark of BCR inhibitors in CLL.<sup>23,25,32,33</sup> Here we report clinical and biological aspects of ibrutinib-induced lymphocytosis in patients with CLL; we show that the rise in ALC is virtually immediate, driven by the efflux of cells from tissue compartments, and paralleled by a substantial decrease in total tumor burden. In prospective

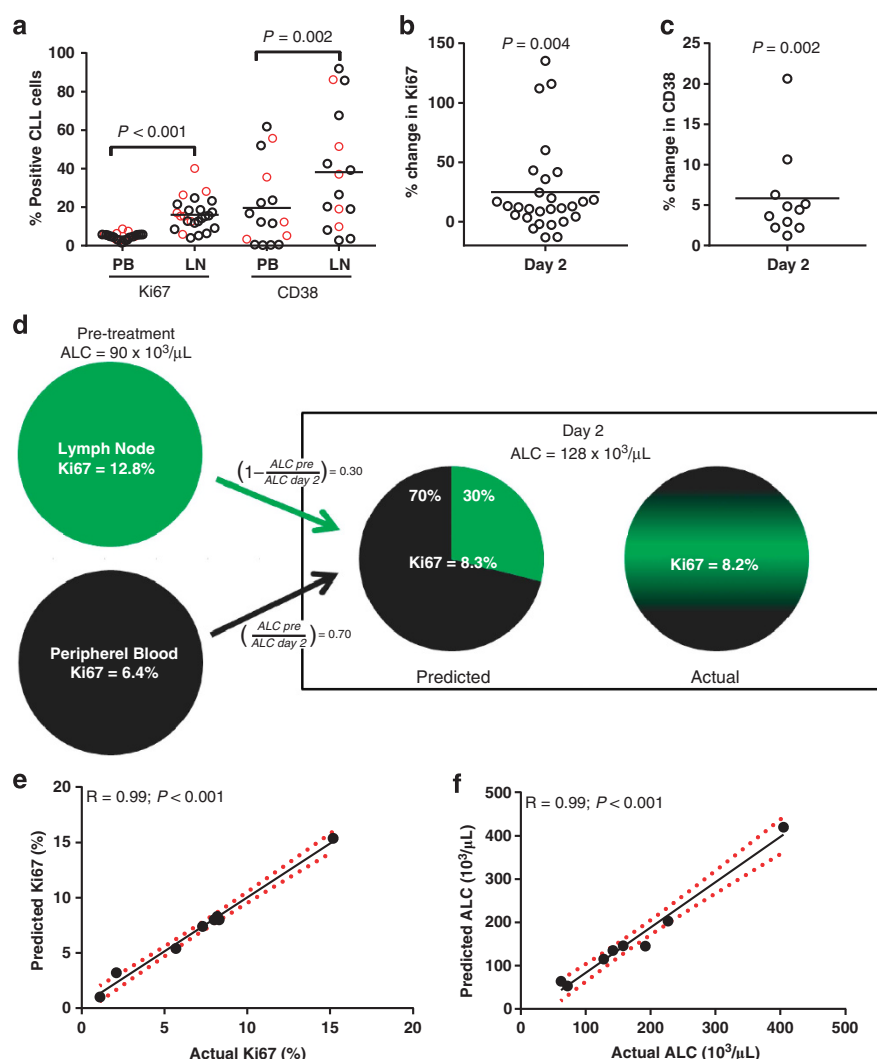


**Figure 4.** Ibrutinib-induced lymphocytosis is driven by the release of cells from the LN. (a) More CLL cells in the LN express Ki67 (proliferation marker) and CD38 (activation marker) compared with CLL cells in the PB. All data are from untreated patients, red symbols represent ibrutinib study patients ( $n = 5$ ). (b) Shown is the relative change in the frequency of Ki67-positive CLL cells in the PB on day 2 (after one dose of ibrutinib) compared with pretreatment ( $n = 28$ ). (c) Change in the frequency of CD38-positive CLL cells on day 2 compared with pretreatment ( $n = 11$ , CD38+ patients only). (d) Efflux of CLL cells from the LN increases the fraction of Ki67-positive cells in the blood. Shown is the data for one representative patient. The frequency of Ki67-expressing CLL cells before treatment in the LN (measured in single-cell suspension by flow cytometry) and in the PB is shown. On day 2, 30% of the ALC consists of 'additional cells' and the frequency of Ki67-positive CLL cells has increased to 8.2%. If all the additional cells are derived from the LN (with Ki67 expression in 12.8%), the predicted frequency of Ki67-positive cells is 8.3%. (e, f) Regression analysis of predicted vs actual percentage of Ki67 expression (e) and ALC values (f). Dashed lines indicate 95% confidence intervals ( $n = 8$ ).

measurements of whole-blood viscosity, we identified a small subset of patients in whom whole-blood viscosity can exceed the normal range. However, no clinical adverse events were attributed to the lymphocytosis.

Previous studies have reported treatment-induced lymphocytosis with BCR inhibitors within weeks of initiating treatment.<sup>23,25,33</sup> Here we show the onset of lymphocytosis occurs within hours of the first dose of ibrutinib and identify a group of patients in whom the lymphocytosis peaks within the first days and resolves before the end of the first cycle. The variability in degree and kinetics of the ibrutinib-induced lymphocytosis in our cohort appears to be somewhat more heterogeneous than seen in other studies. Although we included both treatment naive and relapsed/refractory patients of all age groups, and a large proportion of patients having del(17p), none of these characteristics predicted kinetics or degree of lymphocytosis. Of practical consequence is the observation that patients with a high pretreatment ALC tend

to have a rapid but relatively modest rise in ALC followed by fast resolution of the leukemic disease. Conversely, the group of patients showing a slow but continuous rise in ALC also had slow resolution of leukemic disease, had lower ALC before treatment, a higher proportion of patients with bulky disease and commonly had *IGHV*-mutated CLL. Thus, patients in this group would be predicted to have a more indolent course and extended benefit of treatment, at least with conventional chemoimmunotherapy.<sup>1,49</sup> Therefore, as long as there is no evidence of progressive disease in other sites, it seems appropriate to continue treatment and await the eventual resolution of the lymphocytosis. Overall, compared with patients with *IGHV*-unmutated CLL, patients with *IGHV*-mutated CLL had a greater relative increase in ALC and slower resolution of lymphocytosis, confirming an earlier report.<sup>25</sup> Although *IGHV*-mutated patients may therefore have lower response rates by IWCLL (International Workshop on Chronic Lymphocytic Leukemia) criteria, Woyach *et al.*<sup>38</sup> recently showed

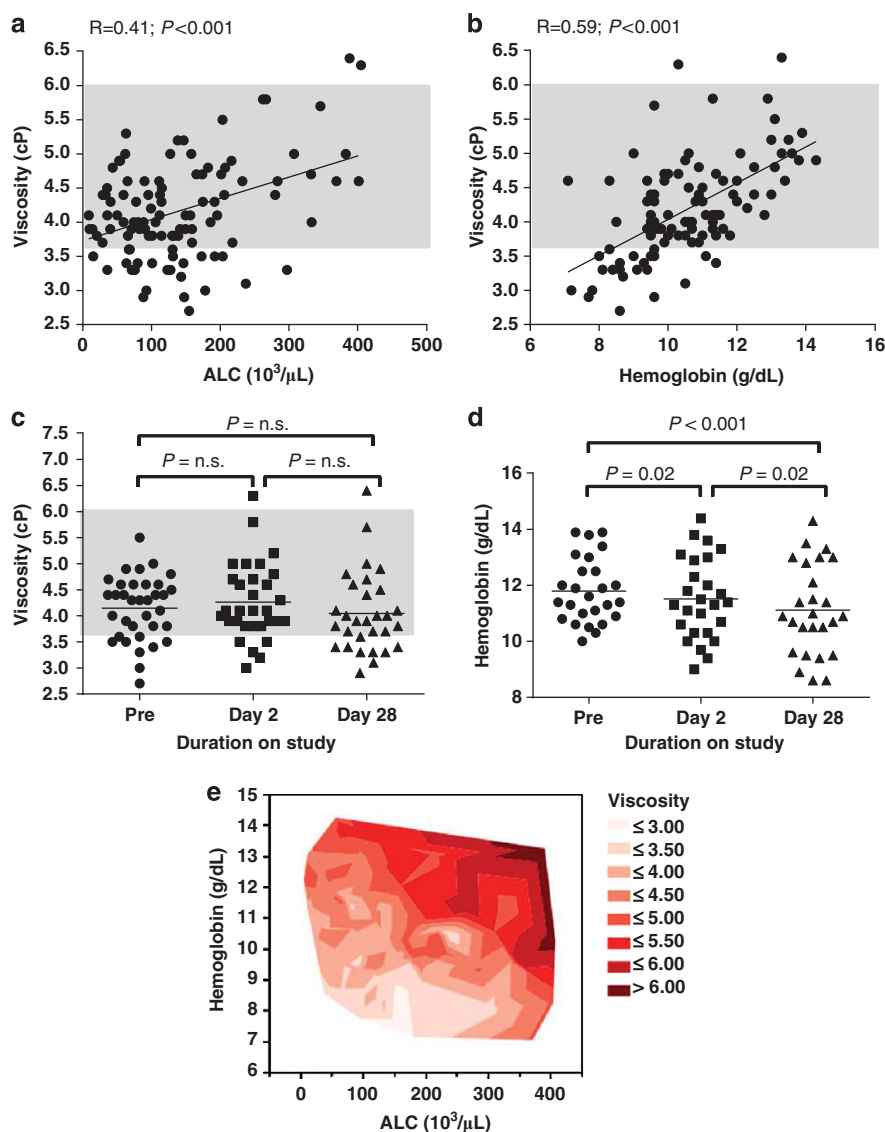


**Figure 5.** Whole-blood viscosity is rarely elevated in CLL and is influenced by ALC and hemoglobin. **(a)** Correlation of whole-blood viscosity (normal range 3.6–6 cP, shaded) with ALC ( $n = 105$ ;  $R = 0.41$ ;  $P < 0.001$ ). **(b)** Correlation of whole-blood viscosity with hemoglobin concentration ( $n = 105$ ;  $R = 0.59$ ;  $P < 0.001$ ). **(c)** Whole-blood viscosity before treatment (Pre) and on treatment days 2 and 28. **(d)** Change in hemoglobin in patients with an initial value  $\geq 10$  g/dl ( $n = 26$ ). **(e)** Contour plot of whole-blood viscosity as a function of both ALC and hemoglobin. Whole-blood viscosity measurements are color coded from low (white) to high (red). Correlations by Pearson's test.

that patients with persistent lymphocytosis have a similar progression-free survival compared with those who reach an IWCLL objective response within the first year. In accordance with this, we did not find a significant difference in the degree of nodal response at 6 months among the three clusters, further suggesting that a prolonged lymphocytosis does not indicate an inferior response.

Resolution of lymphadenopathy concurrent with the rise in ALC has been a strong indication that treatment-induced lymphocytosis is not a sign of progressive disease but reflects redistribution of tumor cells between different anatomical compartments.<sup>7,23,25</sup> Here we present, for the first time, direct evidence that the initial rapid rise in ALC is driven by the release of CLL cells from tissues, in particular from the LN. This conclusion is based on the increased frequency of CLL cells expressing Ki67 and CD38 in the blood within 24 h of starting ibrutinib and supported by a mathematical model derived from *in vivo* measurements in both blood and LN-resident cells (Figure 4d). At least in the first 24 h, the bulk of cells released into the blood appear to come from

the LN, but we cannot rule out that some cells also egress from the bone marrow or other tissue sites. Although several markers have been reported to be differentially expressed among CLL cells in the blood and tissues,<sup>13,42,43</sup> not all are suitable to assess shifts in cell populations on ibrutinib. For example, the activation markers CD69 and CD86 are so rapidly downregulated by ibrutinib that they cannot identify different cell populations once treatment is initiated. In contrast, we observed an increase of CXCR4 expression on CLL cells during treatment with ibrutinib (data not shown), which precludes the identification of the CXCR4<sup>dim</sup>/CD5<sup>bright</sup> population reported by Calissano *et al.*<sup>50</sup> Similarly, on continued treatment both Ki67 and CD38 are downregulated by BCR inhibitors.<sup>45–47</sup> Therefore, we could not distinguish different cell populations at later time points. Thus, while we show that an efflux of cells from the tissue into the blood accounted for the observed rise in ALC by day 2, we cannot assess to what degree reduced homing of CLL cells to the tissue may contribute to the persistence of the lymphocytosis. However, the latter mechanism may contribute to the drop in ALC during

treatment interruptions as seen in early studies that cycled ibrutinib 4 weeks on, one week off.<sup>23,25</sup>

Leukostasis is a rarely reported complication of CLL.<sup>51</sup> However, in some settings the treatment-induced worsening of lymphocytosis has raised concerns about patient safety. We therefore prospectively incorporated whole-blood viscosity measurements. Clinically, we did not observe any symptoms or signs suggestive of leukostasis. Further, whole-blood viscosity was only slightly elevated in two patients. Although our experience is limited in patients with ALC > 300 000/ $\mu$ l, the positive correlation between ALC and whole-blood viscosity suggests that blood flow may be altered at very high ALCs, especially in patients with normal hemoglobin (Figure 5e). The fact that most patients with high ALC had hemoglobin < 10 g/dl could, in part, account for their normal viscosity readings and may justify withholding administration of blood products in patients with high ALC.

Treatment-induced lymphocytosis has attracted considerable attention. However, in most patients, the circulating CLL cells are only a minor fraction of the total tumor volume. Importantly, the bulk of the disease, located in tissue sites such as the bone marrow, LN, spleen and likely the intestinal tract,<sup>39,40</sup> is substantially decreased on ibrutinib (Figure 3). Also, 27% of patients already had a reduction in ALC below baseline by 2 weeks. Thus, in most patients there is a rapid reduction in total tumor burden, indicating an increased rate of cell death on ibrutinib. In fresh whole-blood samples obtained before treatment, we identified a median 2.4% of the circulating tumor cells as dead or dying, which is within the range of the previously calculated daily death rates in untreated CLL patients using heavy water labeling.<sup>42</sup> Our measurements suggest that the frequency of dead or dying cells in circulation more than doubled on ibrutinib (Figure 3f). As dead cells are constantly cleared through the reticuloendothelial system, this is most consistent with an increased death rate. An absolute increase in the rate of cell death by 2% per day would result in a > 50% reduction in tumor burden within 28 days, which is in good agreement with the initial kinetics of tumor response seen in many patients. In addition, inhibition of tumor proliferation by ibrutinib, as reported elsewhere,<sup>46,47</sup> will prevent or reduce the replacement of the dying cells. A slow but steady decay rate of the tumor is also in accordance with the notable absence of reports of tumor lysis syndrome with single agent ibrutinib<sup>23,25</sup> and the modest degree of apoptosis induced by ibrutinib *in vitro*.<sup>26,28</sup> As BCR inhibitors decrease nuclear factor- $\kappa$ B signaling and expression of the anti-apoptotic BCL2 family member BCL2A1,<sup>30,45,46</sup> cell death may be a consequence of reduced pro-survival signaling rather than of a direct cytotoxic effect. However, this remains to be more fully evaluated.

Ibrutinib is active in several mature B-cell malignancies.<sup>23,52</sup> Notably, patients with mantle cell lymphoma also frequently experience treatment-induced lymphocytosis.<sup>44,52</sup> Although the mechanisms leading to redistribution of disease may be similar to those in CLL, patterns of lymphocytosis in mantle cell lymphoma and their relation to clinical response and patient safety need to be independently studied. Results presented here support the positive benefit to risk profile of continued ibrutinib treatment for most patients with CLL showing treatment-induced lymphocytosis. In fact, treatment-induced lymphocytosis in CLL may be viewed as an on-target effect of BCR inhibitors, with the caveat that it may be missed as the peak can occur within the first days or even hours of starting ibrutinib. Thus treatment-induced lymphocytosis is neither a sign of progressive disease nor can it be used as a surrogate of response.

## CONFLICT OF INTEREST

CHG obtained research funding from Genzyme/Sanofi and is on advisory boards for Roche, Janssen, Celgene and GlaxoSmithKline. The other authors declare no conflict of interest.

## ACKNOWLEDGEMENTS

We thank our patients for participating and donating samples to make this research possible. We thank Ajunae Wells for assistance in the clinic and Stephanie Housel, Adrian Byrnes and Allison Wise for protocol support. We acknowledge Pharmacyclics for providing study drug. This work was supported by the Intramural Research Program of NHLBI, NIH. CUN was supported by The Danish Cancer Society. JJ was supported by the NIH Medical Research Scholars Program, a public-private partnership supported jointly by the NIH and generous contributions to the Foundation for the NIH from Pfizer Inc, The Leona M and Harry B Helmsley Charitable Trust and the Howard Hughes Medical Institute, as well as other private donors (<http://www.fnih.org/work/programs-development/medical-research-scholars-program>).

## AUTHOR CONTRIBUTIONS

SEMh, CUN and MF planned the research, performed experiments and analyzed data; JJ, RZM, AL, NS, CHG and SM were involved in planning and supporting components of the research; JG and LBP determined *IGHV* mutational status; IM and KRC performed pathology review; DL conducted statistical analyses; AW planned and supervised the research; and MF, SS, JV, GA, SM, GEM and AW implemented the clinical trial. SEMh, CUN and AW wrote the paper, with all the authors approving the final version.

## REFERENCES

- Chiorazzi N, Rai KR, Ferrarini M. Chronic lymphocytic leukemia. *N Engl J Med* 2005; **352**: 804–815.
- NIH. *NCI Surveillance Epidemiology and End Results*. Department of Health & Human Services: Bethesda, MD, USA, 2012. [seer.cancer.gov](http://seer.cancer.gov).
- Howlader N, Ries LA, Mariotto AB, Reichman ME, Ruhl J, Cronin KA. Improved estimates of cancer-specific survival rates from population-based data. *J Natl Cancer Inst* 2010; **102**: 1584–1598.
- Wierda WG, O'Brien S, Wang X, Faderl S, Ferrajoli A, Do KA *et al*. Prognostic nomogram and index for overall survival in previously untreated patients with chronic lymphocytic leukemia. *Blood* 2007; **109**: 4679–4685.
- Rosenquist R, Cortese D, Bhoi S, Mansouri L, Gunnarsson R. Prognostic markers and their clinical applicability in chronic lymphocytic leukemia: where do we stand? *Leuk Lymphoma* 2013; **54**: 2351–2364.
- Stevenson FK, Krysov S, Davies AJ, Steele AJ, Packham G. B-cell receptor signaling in chronic lymphocytic leukemia. *Blood* 2011; **118**: 4313–4320.
- Wiestner A. Emerging role of kinase-targeted strategies in chronic lymphocytic leukemia. *Blood* 2012; **120**: 4684–4691.
- Woyach JA, Johnson AJ, Byrd JC. The B-cell receptor signaling pathway as a therapeutic target in CLL. *Blood* 2012; **120**: 1175–1184.
- Fais F, Ghiotto F, Hashimoto S, Sellars B, Valetto A, Allen SL *et al*. Chronic lymphocytic leukemia B cells express restricted sets of mutated and unmutated antigen receptors. *J Clin Invest* 1998; **102**: 1515–1525.
- Tobin G, Thunberg U, Karlsson K, Murray F, Laurell A, Willander K *et al*. Subsets with restricted immunoglobulin gene rearrangement features indicate a role for antigen selection in the development of chronic lymphocytic leukemia. *Blood* 2004; **104**: 2879–2885.
- Messmer BT, Albesiano E, Efremov DG, Ghiotto F, Allen SL, Kolitz J *et al*. Multiple distinct sets of stereotyped antigen receptors indicate a role for antigen in promoting chronic lymphocytic leukemia. *J Exp Med* 2004; **200**: 519–525.
- Agathangelidis A, Darzentas N, Hadzidimitriou A, Brochet X, Murray F, Yan XJ *et al*. Stereotyped B-cell receptors in one-third of chronic lymphocytic leukemia: a molecular classification with implications for targeted therapies. *Blood* 2012; **119**: 4467–4475.
- Herishanu Y, Perez-Galan P, Liu D, Biancotto A, Pittaluga S, Vire B *et al*. The lymph node microenvironment promotes B-cell receptor signaling, NF- $\kappa$ B activation, and tumor proliferation in chronic lymphocytic leukemia. *Blood* 2011; **117**: 563–574.
- Burger JA, Ghia P, Rosenwald A, Caligaris-Cappio F. The microenvironment in mature B-cell malignancies: a target for new treatment strategies. *Blood* 2009; **114**: 3367–3375.
- Niemann CU, Wiestner A. B-cell receptor signaling as a driver of lymphoma development and evolution. *Semin Cancer Biol* 2013; **23**: 410–421.
- Young RM, Staudt LM. Targeting pathological B cell receptor signalling in lymphoid malignancies. *Nat Rev Drug Discov* 2013; **12**: 229–243.
- Buggy JJ, Elias L. Bruton tyrosine kinase (BTK) and its role in B-cell malignancy. *Int Rev Immunol* 2012; **31**: 119–132.
- Humphries LA, Dangelmaier C, Sommer K, Kipp K, Kato RM, Griffith N *et al*. Tec kinases mediate sustained calcium influx via site-specific tyrosine



- phosphorylation of the phospholipase Cgamma Src homology 2-Src homology 3 linker. *J Biol Chem* 2004; **279**: 37651–37661.
- 19 Davis RE, Ngo VN, Lenz G, Tolar P, Young RM, Romesser PB *et al*. Chronic active B-cell-receptor signalling in diffuse large B-cell lymphoma. *Nature* 2010; **463**: 88–92.
  - 20 Woyach JA, Bojnik E, Ruppert AS, Stefanovski MR, Goettl VM, Smucker KA *et al*. Bruton's tyrosine kinase (BTK) function is important to the development and expansion of chronic lymphocytic leukemia (CLL). *Blood* 2013; **123**: 1207–1213.
  - 21 Kil LP, de Bruijn MJ, van Hulst JA, Langerak AW, Yuvaraj S, Hendriks RW. Bruton's tyrosine kinase mediated signaling enhances leukemogenesis in a mouse model for chronic lymphocytic leukemia. *Am J Blood Res* 2013; **3**: 71–83.
  - 22 Pan Z, Scheerens H, Li SJ, Schultz BE, Sprengeler PA, Burrill LC *et al*. Discovery of selective irreversible inhibitors for Bruton's tyrosine kinase. *Chem Med Chem* 2007; **2**: 58–61.
  - 23 Advani RH, Buggy JJ, Sharman JP, Smith SM, Boyd TE, Grant B *et al*. Bruton tyrosine kinase inhibitor ibrutinib (PCI-32765) has significant activity in patients with relapsed/refractory B-cell malignancies. *J Clin Oncol* 2013; **31**: 88–94.
  - 24 Wiestner A. Targeting B-Cell receptor signaling for anticancer therapy: the Bruton's tyrosine kinase inhibitor ibrutinib induces impressive responses in B-cell malignancies. *J Clin Oncol* 2013; **31**: 128–130.
  - 25 Byrd JC, Furman RR, Coutre SE, Flinn IW, Burger JA, Blum KA *et al*. Targeting BTK with ibrutinib in relapsed chronic lymphocytic leukemia. *N Engl J Med* 2013; **369**: 32–42.
  - 26 Herman SE, Gordon AL, Hertlein E, Ramanunni A, Zhang X, Jaglowski S *et al*. Bruton tyrosine kinase represents a promising therapeutic target for treatment of chronic lymphocytic leukemia and is effectively targeted by PCI-32765. *Blood* 2011; **117**: 6287–6296.
  - 27 de Rooij MF, Kuil A, Geest CR, Eldering E, Chang BY, Buggy JJ *et al*. The clinically active BTK inhibitor PCI-32765 targets B-cell receptor- and chemokine-controlled adhesion and migration in chronic lymphocytic leukemia. *Blood* 2012; **119**: 2590–2594.
  - 28 Ponader S, Chen SS, Buggy JJ, Balakrishnan K, Gandhi V, Wierda WG *et al*. The Bruton tyrosine kinase inhibitor PCI-32765 thwarts chronic lymphocytic leukemia cell survival and tissue homing in vitro and in vivo. *Blood* 2012; **119**: 1182–1189.
  - 29 de Gorter DJ, Beuling EA, Kersseboom R, Middendorp S, van Gils JM, Hendriks RW *et al*. Bruton's tyrosine kinase and phospholipase Cgamma2 mediate chemokine-controlled B cell migration and homing. *Immunity* 2007; **26**: 93–104.
  - 30 Herman SE, Sun X, McAuley EM, Hsieh MM, Pittaluga S, Raffeld M *et al*. Modeling tumor-host interactions of chronic lymphocytic leukemia in xenografted mice to study tumor biology and evaluate targeted therapy. *Leukemia* 2013; **27**: 1769–1773.
  - 31 Davids MS, Brown JR. Targeting the B cell receptor pathway in chronic lymphocytic leukemia. *Leuk Lymphoma* 2012; **53**: 2362–2370.
  - 32 Cheson BD, Byrd JC, Rai KR, Kay NE, O'Brien SM, Flinn IW *et al*. Novel targeted agents and the need to refine clinical end points in chronic lymphocytic leukemia. *J Clin Oncol* 2012; **30**: 2820–2822.
  - 33 Friedberg JW, Sharman J, Sweetenham J, Johnston PB, Vose JM, Lacasce A *et al*. Inhibition of Syk with fostamatinib disodium has significant clinical activity in non-Hodgkin lymphoma and chronic lymphocytic leukemia. *Blood* 2010; **115**: 2578–2585.
  - 34 Zhang B, Lewis SM. The splenomegaly of myeloproliferative and lymphoproliferative disorders: splenic cellularity and vascularity. *Eur J Haematol* 1989; **43**: 63–66.
  - 35 Sambucetti G, Brignone M, Marini C, Massollo M, Fiz F, Morbelli S *et al*. Estimating the whole bone-marrow asset in humans by a computational approach to integrated PET/CT imaging. *Eur J Nucl Med Mol Imaging* 2012; **39**: 1326–1338.
  - 36 Pesic V, Plecas-Solarovic B, Radojevic K, Kosec D, Pilipovic I, Perisic M *et al*. Long-term beta-adrenergic receptor blockade increases levels of the most mature thymocyte subsets in aged rats. *Int Immunopharmacol* 2007; **7**: 674–686.
  - 37 Nadler SB, Hidalgo JH, Bloch T. Prediction of blood volume in normal human adults. *Surgery* 1962; **51**: 224–232.
  - 38 Woyach JA, Smucker K, Smith LL, Lozanski A, Zhong Y, Ruppert AS *et al*. Prolonged lymphocytosis during ibrutinib therapy is associated with distinct molecular characteristics and does not indicate a suboptimal response to therapy. *Blood* 2014; **123**: 1810–1817.
  - 39 Kuse R, Lueb H. Gastrointestinal involvement in patients with chronic lymphocytic leukemia. *Leukemia* 1997; **11**(Suppl 2): S50–S51.
  - 40 Baumhoer D, Tzankov A, Dirnhofer S, Tornillo L, Terracciano LM. Patterns of liver infiltration in lymphoproliferative disease. *Histopathology* 2008; **53**: 81–90.
  - 41 Brandtzaeg P, Farstad IN, Johansen FE, Morton HC, Norderhaug IN, Yamanaka T. The B-cell system of human mucosae and exocrine glands. *Immunol Rev* 1999; **171**: 45–87.
  - 42 Messmer BT, Messmer D, Allen SL, Kolitz JE, Kudalkar P, Cesar D *et al*. In vivo measurements document the dynamic cellular kinetics of chronic lymphocytic leukemia B cells. *J Clin Invest* 2005; **115**: 755–764.
  - 43 Calissano C, Damle RN, Hayes G, Murphy EJ, Hellerstein MK, Moreno C *et al*. In vivo intracloal and interclonal kinetic heterogeneity in B-cell chronic lymphocytic leukemia. *Blood* 2009; **114**: 4832–4842.
  - 44 Chang BY, Francesco M, De Rooij MF, Magadala P, Steggerda SM, Huang MM *et al*. Egress of CD19+CD5+ cells into peripheral blood following treatment with the Bruton tyrosine kinase inhibitor ibrutinib in mantle cell lymphoma patients. *Blood* 2013; **122**: 2412–2424.
  - 45 Herman SE, Barr PM, McAuley EM, Liu D, Wiestner A, Friedberg JW. Fostamatinib inhibits B-cell receptor signaling, cellular activation and tumor proliferation in patients with relapsed and refractory chronic lymphocytic leukemia. *Leukemia* 2013; **27**: 1769–1773.
  - 46 Herman SEM, Farooqui M, Bezabhe R, Aue G, Wiestner A. In vivo effects of ibrutinib on BCR signaling, tumor cell activation and proliferation in blood and tissue-resident cells of chronic lymphocytic leukemia patients. *ASH Annu Meeting Abstracts* 2012; **120**: 185.
  - 47 Cheng S, Ma J, Guo A, Lu P, Leonard JP, Coleman M *et al*. BTK inhibition targets in vivo CLL proliferation through its effects on B-cell receptor signaling activity. *Leukemia* 2013; **28**: 649–657.
  - 48 Ganzel C, Becker J, Mintz PD, Lazarus HM, Rowe JM. Hyperleukocytosis, leukostasis and leukapheresis: practice management. *Blood Rev* 2012; **26**: 117–122.
  - 49 Tam CS, O'Brien S, Wierda W, Kantarjian H, Wen S, Do KA *et al*. Long-term results of the fludarabine, cyclophosphamide, and rituximab regimen as initial therapy of chronic lymphocytic leukemia. *Blood* 2008; **112**: 975–980.
  - 50 Calissano C, Damle RN, Marsilio S, Yan XJ, Yancopoulos S, Hayes G *et al*. Intracloal complexity in chronic lymphocytic leukemia: fractions enriched in recently born/divided and older/quiescent cells. *Mol Med* 2011; **17**: 1374–1382.
  - 51 Cukierman T, Gatt ME, Libster D, Goldschmidt N, Matzner Y. Chronic lymphocytic leukemia presenting with extreme hyperleukocytosis and thrombosis of the common femoral vein. *Leuk Lymphoma* 2002; **43**: 1865–1868.
  - 52 Wang ML, Rule S, Martin P, Goy A, Auer R, Kahl BS *et al*. Targeting BTK with ibrutinib in relapsed or refractory mantle-cell lymphoma. *N Engl J Med* 2013; **369**: 507–516.

Supplementary Information accompanies this paper on the Leukemia website (<http://www.nature.com/leu>)